PCCP

Accepted Manuscript

ROYAL SOCIETY OF CHEMISTRY

www.rsc.org/pccp

Interactional Behavior of Polyelectrolyte Poly Sodium 4-Styrene Sulphonate (NaPSS) with Imidazolium based Surface Active Ionic Liquids in Aqueous Medium

Renu Sharma, Ajar Kamal, Tejwant Singh Kang*, Rakesh Kumar Mahajan*

[*]Department of Chemistry, UGC-Centre for Advanced Studies-I, Guru Nanak Dev University, Amritsar-143005, India

**To whom correspondence should be addressed:*

e-mail: rakesh_chem@yahoo.com; tejwantsinghkang@gmail.com; Fax: +91 183 2258820

Abstract

The present study aims to develop an understanding of the interactions between anionic polyelectrolyte; poly sodium 4-styrene sulphonate (NaPSS) and cationic surface active imidazolium based ionic liquids (SAILs), [$C_n$mim][Cl] (n = 10, 12, 14) using multi-technique approach. Various physico-chemical and electrochemical techniques such as surface tension, conductivity, fluorescence, isothermal titration calorimetry (ITC), dynamic light scattering (DLS), turbidity, potentiometry, cyclic voltammetry (CV), and differential pulse voltammetry (DPV) are employed to get a comprehensive information about NaPSS-SAILs interactions. Different stages of interactions corresponding to critical aggregation concentration (*cac*), critical saturation concentration (C_s) and critical micelle concentration (*cmc*) have been observed owing to strong electrostatic and hydrophobic interactions and the results obtained from different techniques complement each other, very well. The results extracted from DLS and turbidity measurements clearly indicated that the size of the micelle like aggregates first decreases and then, increases in the presence of polyelectrolyte. The binding isotherms obtained using potentiometry show a concentration dependence and highly co-operative nature of interactions which is attributed to aggregation of the polyelectrolyte-SAIL complexes. Diffusion coefficients (D_m) of the electroactive probe in the pure and NaPSS-SAILs mixed systems were obtained which are further used to obtain the values of the micellar self-diffusion coefficients (D^0_m) and inter-micellar interaction parameters (k_d).

Keywords: Poly (sodium 4-styrene sulphonate), Cyclic Voltammetry, Potentiometric sensor, Electrostatic interactions, Micellization, Self-diffusion coefficient.

1. Introduction

The physicochemical and rheological behavior of polyelectrolytes is governed by charge distribution on the polymer chain. The structural and confirmation flexibility of polyelectrolytes in aqueous solutions are attributed mainly to varying degree of ionization and hydrophobic interactions. The mixtures of polyelectrolytes with oppositely charged surfactants in aqueous medium have gained huge attention in the past few decades from the scientific and technological point of view. These mixed systems have a wide era of applications in personal care products, agricultural and pharmaceutical industries [1-5]. In this regard, many research groups have investigated the interactions between polyelectrolytes and oppositely charged surfactants [6-9]. J. Mata *et. al,* [10] have explored the complexation behavior of cationic surfactants of varying chain length and head groups with semi-flexible anionic polyelectrolyte carboxymethylcellulose using surface tension, viscosity, potentiometry and dynamic light scattering techniques. The critical aggregation concentration, *cac* and other characteristic parameters depicting the extent of interactions have been found to be dependent on alkyl chain length and the nature of head group. Staples and coworkers have investigated the interactions between anionic surfactant sodium dodecyl sulphate (SDS) and cationic polymer poly (dimethyldiallylammonium chloride) using surface tension and neutron reflection measurements [11]. Both the measurements revealed that polymer-surfactant mixtures undergo adsorption and desorption processes at the air-solution interface. The strong affinity between polyions and surfactant molecules has been ascribed to electrostatic and hydrophobic interactions.

Poly sodium 4-styrene sulphonate (NaPSS) is water soluble anionic polyelectrolyte bearing aromatic, benzenesulphonate side groups, which adds to its hydrophobicity. Low molecular weight NaPSS undergo self-aggregation in its aqueous solution whereas, high molecular weight NaPSS do not exhibit such behavior. A few literature reports related to the interactions of NaPSS with cationic surfactants are available [12-15]. In this regard, Loh *et al.* has investigated the interactions of polyelectrolyte (NaPSS) and non-ionic polymer (PEO) with zwitterionic surfactants by isothermal titration calorimetry and concluded that different polymers interact in diverse manners with zwitterionic surfactants at different temperatures [15]. Similarly, Wang and Wang have studied the interactions between cationic gemini and single chain

surfactants with anionic polyelectrolytes NaPSS and poly (sodium acrylate) (NaPAA) of different molar masses using isothermal titration calorimetry, turbidity and steady-state fluorescence measurements [16]. They observed that interactional behavior of NaPSS depends on polyelectrolyte molar mass. Kogej and Skerjanc have revealed the aggregation behavior of alkyltrimethylammonium surfactants in aqueous NaPSS solutions using fluorescence and conductivity techniques and concluded that NaPSS induces micelle formation of surfactants at concentration much lower than their critical micelle concentration [17].

On the other hand, ionic liquids (ILs) have been considered as environment friendly solvents having potential to replace volatile organic solvents for a variety of applications [18-20]. One such important aspect of many of the ILs is their inherent amphiphilicity, which places them in the class of ionic surfactants. Therefore, many of the ILs have been investigated for their self-assembly behavior, where, some of them have been found to be better surfactants as compared to conventional ionic surfactants [21-23]. Thereafter, ILs exhibiting surface active nature will be termed as surface active ionic liquids (SAILs). Till now, these SAILs have been explored in conjunction with a variety of polymers and biopolymers [24-29], however there exist only a few reports depicting the interactions between SAILs and polyelectrolytes [30, 31]. The main objective of the present work is to provide basic information about the interactions between ionic liquids and anionic polyelectrolyte, NaPSS. Since, ILs exhibit better surface active properties over the conventional ionic surfactants, it is expected that ILs would show diverse interactional behavior with NaPSS. The results from this work will provide new information from academic point of view. Further, improved colloidal properties of NaPSS in the presence of ILs can find a place in different applications of interest. Recently, B. Das and group [32] have reported the interactions between sodium carboxymethyl cellulose (NaCMC) and SAIL, 1-hexadecyl-3-methylimidazolium chloride (C_{16}MeImCl) using electrical conductivity and surface tension measurements. They explored the aggregation behavior and thermodynamics of SAIL at different temperatures in presence of NaCMC. However, to best of our knowledge, interactions between SAILs, 1-alkyl-3-methylimidazolium chlorides [$C_n$mim][Cl], n = 10, 12, 14 and NaPSS have not been yet explored using different state of art techniques.

In the present work, we have investigated the interactions between surface active ionic liquids (SAILs), 1-alkyl-3-methylimidazolium chlorides, [$C_n$mim][Cl], n = 10, 12, 14 and poly

sodium 4-styrene sulphonate (NaPSS) using surface tension, conductivity, fluorescence, dynamic light scattering (DLS), potentiometry, turbidity, isothermal titration calorimetry (ITC), cyclic voltammetry (CV), and differential pulse voltammetry (DPV) techniques. The aggregation behavior of SAILs in the presence of NaPSS at air-solution interface has been investigated by surface tension measurements. Various surface parameters like surface tension at *cmc* (γ_{cmc}), Gibbs surface excess (Γ_{max}), minimum area per molecule (A_{min}) have been calculated using surface tension data. Thermodynamic parameters of micellization have been deduced using conductivity and ITC measurements. DLS and turbidity measurements have shed light on the size of the complexes formed between NaPSS and SAILs in different concentration regimes. Binding studies between NaPSS and SAILs have been performed using potentiometry. Electrochemical studies (CV and DPV) are performed to understand the aggregation behavior of SAILs and to obtain diffusion coefficient (D_m), self-diffusion coefficient (D^0_m), and inter-micellar interaction parameter (k_d) in the presence of NaPSS.

2. Experimental section

2.1. Materials and methods

The surface active ionic liquids (SAILs), 1-alkyl-3-methylimidazolium chloride [$C_n$mim][Cl] where n = 10, 12 and 14 were prepared by the procedure mentioned elsewhere in he literature [33] and then characterized by ^{1}H NMR technique. Poly (sodium 4-styrene sulphonate), 1-methyl imidazole, 1-chlorodecane, 1-chlorododecane, 1-chlorotetradecane, poly (sodium 4-styrene sulphonate), fluorescence probe 8-anilino-1-naphthalenesulphonic acid (ANS), and 2, 2, 6, 6-tetramethyl piperidinyloxy (Tempo) with 98% purity were purchased from Sigma Aldrich and used as received. The plasticizer, bis(2-ethyl-hexyl) phthalate (DOP) was a product of Qualigens, India. The molecular structures of SAILs and the polyelectrolyte under investigation are shown in Scheme 1 (a, b). All the solutions were prepared in double distilled water. A sartorius analytical balance with a precision of ± 0.0001 g was used for weighing purpose. For all the measurements, titration method was used and the concentration of polyelectrolyte was kept constant at two different concentrations (0.002% and 0.005%). All the measurements were carried out at 298.15 K, if not stated otherwise. The annexure describing the methodology employed for various measurements in detail is provided as Annexure SI (supporting information).

3. Results

3.1 Surface tension studies of mixed systems of SAILs and NaPSS

Fig. 1(a) and (b) depicts the variation of surface tension (γ) as a function of concentration of surface active ionic liquids (SAILs), [$C_n$mim][Cl] where n = 10, 12, and 14 in aqueous solution of NaPSS at a concentration of 0.002% and for NaPSS-[C_{10}mim][Cl] mixed system at 0.002 and 0.005% of NaPSS concentrations, respectively. The corresponding plots for other mixed systems are provided as supporting information [Fig. S1(a, b)]. The tensiometric profiles of pure SAILs in water show one transition corresponding to critical micelle concentration (*cmc*), as expected. The *cmc* values of SAILs are found to be in good agreement with the literature values [34]. For investigated NaPSS-SAILs mixed systems, a complicated behavior has been observed. The interactions of SAIL monomers with NaPSS molecules exhibit convoluted behavior depending on the length of alkyl chain of SAILs as can be seen from Fig. 1(a). The presence of polyelectrolyte does not alter the γ value of pure water *i.e.* 72.8 mN m^{-1}, which indicates that NaPSS is not a surface active polymer [35-37]. The tensiometric profiles of NaPSS-SAIL mixed systems show different regimes corresponding to different extent of complexation between NaPSS and SAILs with the increase in concentration of SAILs. Various interfacial and thermodynamic parameters like surface tension at *cmc* (γ_{cmc}), maximum surface excess concentration at the air-solution interface (Γ_{max}), minimum area per molecule (A_{min}), effectiveness of surface tension reduction (π_{cmc}), Gibbs free energy of adsorption (ΔG°_{ads}) (using ΔG°_{mic} from conductivity at 298.15K) have been calculated using the standard equations (Annexure SII, supporting information) and the values are given in Table S1 (supporting information). The values of Γ_{max} for [C_{10}mim][Cl], [C_{12}mim][Cl] and [C_{14}mim][Cl] in aqueous solution are 1.41, 2.08 and 2.27 μmol m^{-2} respectively, which indicates the increasing adsorption efficiency of SAIL with increase in alkyl chain length. The same trend of variation in Γ_{max} values have been observed in the presence of polyelectrolyte. However, Γ_{max} values have been found to be higher at higher concentration of NaPSS, which reveals the formation of stable and compact surface active NaPSS-SAIL (aggregate) complex at the air-solution interface. The A_{min} values show opposite behavior to that of Γ_{max} for different SAILs as expected [38]. The ΔG°_{ads} values are more negative than ΔG°_{mic} values which indicate the spontaneity of adsorption process over

micellization. However, the values of ΔG°_{ads} become less negative with the increase in concentration of NaPSS from 0.002% to 0.0005% in the studied mixed systems.

3.2 Conductivity measurements

In order to determine *cmc* by conductivity technique, the aggregates of micelles formed in bulk must possess a structure of suitable composition to provide an aggregate having degree of dissociation other than unity and that is accountable for a clear break in plots of conductivity (κ) versus concentration of surfactant [39]. The conductivity measurements have been carried out at four different temperatures ranging from 298.15-313.15 K. The plots showing the variation of conductivity (κ) as a function of concentration of $[C_{10}mim][Cl]$ in aqueous NaPSS solution at concentrations of 0.002 and 0.005% of NaPSS are shown in Fig. 2(a, b), respectively, and the respective plots for pure SAILs and other NaPSS-SAIL mixed systems are provided as supporting information [Fig. S2, S3 and S4]. The change in conductivity values for pure SAILs fit into two straight lines of different slopes and the point of intersection of the lines of the abrupt change in slopes gives the value of *cmc*. Initially below *cmc*, free mobile ions of SAILs are responsible for sharp increase inκ, whereas after *cmc*, micelles are formed which contribute less towards the charge transport leading to smaller slopes in conductivity profiles. The conductivity profiles of NaPSS-SAILs systems show three lines of different slopes S_1, S_2 and S_3, whose intersection points corresponds to two transitions designated as *cac* and *cmc* of SAILs. The magnitude of three slopes follow the order $S_1 > S_2 > S_3$. The clear picture of two intersection points is shown in inset of the Fig. 2(a, b). The degree of counter-ion binding (β) provides the average number of counter-ions per surfactant ions in the micelle and is related to related to degree of dissociation (α) as $\beta = 1-\alpha$ [40], where α is obtained by the ratio of slopes of conductivity profiles in post to pre-micellar region. The values of *cmc* and β of SAILs in aqueous and aqueous polyelectrolyte solutions are given in Tables S2, S3, and S4 respectively (supporting data). The *cmc* values of pure SAILs have been found to be in good agreement with their literature values and with those obtained from other techniques employed. Various thermodynamic parameters like Gibbs free energy (ΔG_{mic}), enthalpy (ΔH_{mic}) and entropy (ΔS_{mic}) of micelle formation have been calculated using the standard equations (Annexure SIII, supporting information). The calculated thermodynamic parameters of SAILs in aqueous and

aqueous NaPSS solution at 0.002 and 0.005% concentrations of NaPSS are given in Table S2, S3, and S4 (supporting information). The negative values of ΔG_{mic} indicate the spontaneity of the micellization process and their values increase with the increase in alkyl chain length of SAILs, which suggest that the process become more facile with the increase in hydrophobicity of SAILs. ΔG_{mic} become less negative in the presence of polyelectrolyte at both the concentrations (0.002% and 0.005%) for all investigated polyelectrolyte-SAIL mixed systems as compared to that in the absence of polyelectrolyte. This suggests that presence of polyelectrolyte hinders the micellization process to some extent. However, this effect is more pronounced at higher concentration of polyelectrolyte. The large magnitude of $T\Delta S_{mic}$ indicates that micellization process is entropy driven over the investigated temperature range. The $T\Delta S_{mic}$ values increases with the increase in alkyl chain length of SAILs indicating that hydrophobic interactions play an important role in micellization process. However, the values of $T\Delta S_{mic}$ decrease with the increase in concentration of polyelectrolyte from 0.002 to 0.005% in all the mixed systems corroborating the results for other thermodynamic parameters.

3.3 Fluorescence measurements

To get further insights of the interactions between NaPSS and SAILs in the bulk, fluorescence measurements have been performed using 8-anilinonaphthalene sulphonic acid (ANS) as a fluorescent probe. The fluorescent probe ANS, is one of the common hydrophobic probes that possess both a sulphonic acid and amine group. ANS exhibits very low intensity peak in highly polar solvents at 520 nm and intensity increases remarkably with increasing hydrophobicity of the surrounding medium along with shift in fluorescence intensity to 483 nm [17]. The plot of I/I_0 versus concentration gives a measure of *cmc* and relative hydrophobicity of the pure and mixed systems of NaPSS and SAILs, where I_0 and I corresponds to fluorescence intensities of ANS in NaPSS solution and in NaPSS solution with increasing concentration of SAILs. It has been reported that intensity of ANS increases with the increase in hydrophobicity of its micro-environment. In the fluorescence studies using ANS as a probe, the intensity of ANS do not show much increase with the increase in concentration of SAILs, but as concentration approaches *cmc*, there is a sharp increase in intensity which is due to relocation of ANS in the hydrophobic environment of formed micelle. The point of intersection of two lines gives *cmc* of pure SAILs. Such changes in fluorescence intensity of ANS are also reported by Griffiths *et.al* in

which they explored the effect of ethanol on the interactions between nonionic poly(vinylpyrrolidone) (PVP) and an anionic surfactant sodium dodecyl sulphate (SDS) using various techniques [41]. Fig. 3(a) and Fig. S5(a) depicts the fluorescence intensity of ANS in 0.002 and 0.005% NaPSS solution as a function of concentration of three SAILs and Fig. 3(b) gives the fluorescence intensity of ANS in aqueous and aqueous solutions at 0.002 and 0.005% concentrations for NaPSS-[C_{10}mim][Cl]. The obtained *cmc* values of pure SAILs from fluorescence studies compliment well with those obtained from other techniques as well as with that of literature.

3.4 Turbidity and Dynamic Light Scattering (DLS) measurements

To have an idea about the size distribution and morphology of aggregates formed between NaPSS and SAILs at two different concentrations (0.002% and 0.005%) of NaPSS and varying the concentration of SAILs, turbidity and dynamic light scattering measurements have been performed. Fig. 4(a) depicts the turbidity changes for 0.002% NaPSS solution as a function of concentration of investigated SAILs and Fig. 4(b) shows the turbidity changes for NaPSS-[C_{10}mim][Cl] system in 0.002 and 0.005% solutions of NaPSS. The corresponding plots for other mixed systems are provided as supporting information [Fig. S6]. The size distribution curves describing the change in size of different structures formed in NaPSS-SAIL systems as a function of concentration of three SAILs in 0.002% aqueous NaPSS are presented in Fig. 5(a-c) and the corresponding plots for 0.005% concentration of NaPSS are provided as supporting information [Fig. S7(a-c)]. The hydrodynamic diameter (D_h) of NaPSS at a concentration of 0.002% is of ≈105.7 nm, whereas, at a concentration of 0.005%, D_h increases to 164.2 nm which indicates that the polyelectrolyte is not spherical in shape due to repulsive electrostatic interactions in between the charged segments besides the poly-ion chain. The large D_h for 0.005% NaPSS may be due to dimerization of NaPSS molecules.

3.5 Isothermal Titration Calorimetry (ITC) measurements

Isothermal titration calorimetry measurements have been performed to study the heat changes taking place due to various interactions among SAILs and anionic polyelectrolyte, NaPSS in varying concentration regime of SAILs. The enthalpograms of [C_{10}mim][Cl], [C_{12}mim][Cl] and [C_{14}mim][Cl] in the presence and absence of 0.002% and 0.005% aqueous NaPSS solution as a function of concentration of SAIL is shown in Fig. S8(a-c) (supporting

information). The corresponding profiles of differential enthalpy (dP) for SAILs in aqueous and aqueous polyelectrolyte solution (0.005%) are shown in Fig. S8(d-i) respectively (supporting information). From Fig. S8(a-c), it is very much clear that the enthalpograms obtained for aqueous solution of SAILs in the presence of NaPSS are different from that obtained in absence of polyelectrolyte at least in the magnitude, which is ascribed to the binding interactions between polyelectrolyte and SAILs. The enthalpograms can be divided into three concentration regions as shown in Fig. S8(a-c).

4. Discussion

4.1 Interactions in different concentration regimes

The interactions between anionic polyelectrolyte, NaPSS and surface active ionic liquids (SAILs) exhibit three foremost transitions *i.e.* critical aggregation concentration (*cac*), critical saturation concentration (C_s) and critical micelle concentration (*cmc*), which are explored by different physicochemical techniques as described below.

4.1.1 Concentration regime 0 → *cac*

In case of NaPSS-[C_{10}mim][Cl] mixed system, initially, on the addition of SAIL, γ shows sharp decrease from 72.8 to 40 mN m^{-1} and this decrease in γ is assigned to the progressive formation of surface active NaPSS-SAIL (aggregate) complexes at the air-solution interface at low concentration of SAIL called as critical aggregation concentration (*cac*), also designated as C_2. It is important to mention that the transition corresponding to C_1 could not be obtained in this mixed system using tensiometry. The conductivity plots show sharp increase in κ with a higher slope (S_1), which is due to strong electrostatic binding between SAIL monomers and NaPSS molecules and the release of counter-ions upto *cac* (Fig. 2). The fluorescence spectra of ANS in aqueous solution of SAILs show different behavior as compared to that in aqueous NaPSS solutions. In the presence of NaPSS, diverse behavior has been observed by virtue of complexation among NaPSS and SAILs in different concentration regimes. The formation of NaPSS-SAIL (monomer) complexes in bulk similar to that observed at air-solution interface below *cac* creates the hydrophobic patches leading to increased hydrophobicity as sensed by ANS. In addition to these changes, this complexation increases the turbidity [Fig. 4(b)] of the system by the virtue of electrostatic interactions between NaPSS and SAILs, which is supported by decrease in D_h (Fig. 5) from 105.7 to 91.28 nm (0.002% NaPSS) due to contraction of

polyelectrolyte chain. The variation of D_h as a function of concentration of three SAILs in 0.002% NaPSS is represented in Fig. 5(d) and the corresponding plot in 0.005% NaPSS is shown as supporting information [Fig. S7(d)]. The enthalpy changes involved in this regime (C ≤ *cac*) are exothermic in nature as observed from ITC measurements (Fig. S8). Such exothermic enthalpy changes are also observed in rest of the mixed systems in the same concentration regime, where NaPSS-SAIL (monomer) complexes are formed. The exothermic enthalpy changes observed in all NaPSS-SAILs mixed systems may occur due to following interactions: electrostatic interactions between cationic headgroups of SAILs and anionic groups of polyelectrolyte backbone leading to formation of NaPSS-SAIL (monomer) complex, the permeation of benzene rings of NaPSS into the headgroup region of SAILs aggregates and the hydrophobic interactions between alkyl chains of SAILs and hydrophobic moieties of polyelectrolyte. The other reason for such exothermic enthalpy changes may be the inter-chain complexation via hydrogen bonding induced by the binding among fully ionized NaPSS and SAILs similar to that observed in polyacrylic acid and dodecyltrimethylammonium bromide (DTAB) mixed systems [42].

4.1.2 Concentration regime *cac* → C_s

In NaPSS-[C_{10}mim][Cl] mixed system, above *cac*, there occurs a cooperative association of SAIL monomers and NaPSS molecules owing to electrostatic and hydrophobic interactions, which results in some precipitation that usually occur in oppositely charged surfactant-polymer systems [43-46]. Afterwards, γ show negligible change which is due to the saturation of polyelectrolyte backbone by adsorption of more of SAIL molecules between the region *cac* and C_s [Fig. 1(b)]. For NaPSS-[C_{12}mim][Cl] mixed system, beyond *cac*, monomer complex so formed changes to NaPSS-SAIL (aggregate) complex with increase in concentration of SAIL. There is a small increase in γ just below the *cmc*, which is due to dissolution of thus formed non-surface active NaPSS-SAIL (aggregate) complexes in bulk. The concentration corresponding to this transition is termed as critical saturation concentration (C_s). Similar behavior has been observed for NaPSS-[C_{14}mim][Cl] mixed system, but in this system, there is a sharp hump in tensiometric profiles in a narrow and dilute concentration regime [Fig. S1(b)]. The increase in γ and the occurrence of precipitation in the similar concentration range indicates the expulsion of surface active (aggregate) complex from the air-solution interface into to the bulk. However,

enhanced hydrophobic character of NaPSS-[C_{14}mim][Cl] (aggregate) complex due to relatively longer alkyl chain of SAIL may also lead to decreased solubility leading to precipitation in this regime. On the other hand, it is well established that the appearance of such hump in tensiometric profiles of oppositely charged surfactant-polymer systems is due to the competitive formation of three types of complexes. These complexes are: a surface active polymer-surfactant (aggregate) complex (PS_s) at the air-solution interface, another polymer-surfactant (aggregate) complex (PS'_s) formed beneath the initially formed PS_s at air-solution interface and a non-surface active polymer-surfactant (aggregate) complex in the bulk (PS_M), where micelle like structures are formed on the polyelectrolyte backbone leading to formation of necklace-bead like structures. [47]. There is always a competition between the formation of PS'_s and PS_M and the difference in energy gap between the formation of these complexes is responsible for the appearance of hump in the tensiometric profiles as a consequence of dissolution of PS'_s into bulk which further converts to PS_M. This energy gap decreases with the increase in chain length of SAILs by virtue of which, no sub-layer (PS'_s) formation occur for [C_{14}mim][Cl], and for NaPSS-[C_{10}mim][Cl] mixed system, there is no hump in the tensiometric profile since in this case, energy gap among PS'_s and PS_M is quite large and it suggests that PS'_s is more stable than PS_M. Further, there may be the formation of multilayer near the surface which ultimately stabilizes the surface and prevents the presence of hump. The effect of concentration of NaPSS in aqueous solution has also been found to affect the course of interactions between NaPSS and respective SAILs. As the concentration of NaPSS increases from 0.002 to 0.005%, the height of the hump at C_s decreases while following a shift to higher concentrations of respective SAILs in NaPSS-[C_{12}mim][Cl] and -[C_{14}mim][Cl] mixed systems. Such behavior has been reported formerly by some research groups for oppositely charged polyelectrolyte/surfactant mixed systems [47]. In the conductivity measurements, κ increases following a comparatively lower slope after *cac* as compared to that of below *cac* with the addition of SAIL. Hence, the charged sites of polyelectrolyte are neutralized and NaPSS-SAIL (aggregate) complexes are formed due to which slight precipitation occurs and these changes follow a relatively smaller change in conductivity. Thereafter, increase in concentration of SAIL results in dissolution of precipitates of NaPSS-SAIL (aggregate) complexes via enhanced adsorption of added molecules of SAIL onto aggregates and this concentration falls between C_s and *cmc* as observed from tensiometric profiles (Fig. 2).

However, C_s could not be located by conductance as probing of a process by different methods may or may not yield same results. Due to formation of NaPSS-SAIL (aggregate) complexes, the fluorescence intensity of ANS attain a maximum value between C_s and *cmc* indicating no further change in hydrophobicity. As a result, it becomes clear that transitions from monomer to aggregate complexes changes the hydrophobicity of the surroundings sensed by ANS and thus, its intensity increases to reach an utmost value. The fluorescence intensity of ANS increases with the increase in polyelectrolyte concentration in all the NaPSS-SAIL mixed systems as can be seen from Fig. 3(b). It is also interesting that the concentration of SAIL at which maximum occurs in fluorescence intensity coincides with the maximum in turbidity measurements. The turbidity also increases sharply due to cooperative binding of SAIL molecules on polyelectrolyte backbone to approach a maximum value that corresponds to critical saturation (C_s) of polyelectrolyte. Also, at this stage, coecervation takes place leading to increase in turbidity (Fig. 4) and as a result, the size of the aggregates increases from 122 to 712.4 nm as determined using dynamic light scattering (Fig. 5). Therefore, in the investigated NaPSS-SAILs mixed systems, the solutions experience strong electrostatic attractive interactions before complete charge neutralization and afterwards, on complete charge neutralization, electrostatic repulsions come in to play which ultimately affects the structural transformations of the polyelectrolyte. Such changes have also been reported by some research groups for oppositely charged polyelectrolyte-surfactant mixed systems [48, 49]. The schematic representation showing the binding interaction mechanism between NaPSS and SAILs adopted based on the observations made from various techniques is given as scheme 2. In this regime ($cac < C \leq C_s$), the enthalpy changes start increasing and becomes endothermic before reaching a maximum value as can be seen from Fig. S8(c) (supporting information). These endothermic enthalpy changes might be due to the release of counter-ions condensed on charged polymer chains and thus entropy of the system also increases [42].

4.1.3 Concentration regime above C_s

In NaPSS-SAIL mixed systems [Fig. 1(a)], above C_s, γ decreases upto a concentration where free micelles of SAILs begin to form. The concentrations corresponding to all the transitions are listed in Table 1. The different concentrations corresponding to different transitions increase with the increase in concentration of polyelectrolyte from 0.002 to 0.005%. It

is because of the fact that with the increase in concentration of polyelectrolyte, the number of polymer chains in solution increases and thus, more number of SAIL monomers are required to form complex with polyelectrolyte. The *cmc* values in all investigated mixed systems also show an increase with the increase in concentration of polyelectrolyte, which supports the above assumption. The main driving forces responsible for the interactions between NaPSS and SAILs in all investigated systems are electrostatic and hydrophobic interactions. The hydrophobic aromatic side groups attached to polystyrene chains of NaPSS are solubilized near the surface of ionic micelle (near the β-CH_2) group, which are liable for the hydrophobic interactions. Also, it has been reported by NMR measurements that benzene sulphonate groups of NaPSS actively participate in micelle structure [50]. Therefore, the aggregates so formed by the interactions of NaPSS and SAILs in bulk are less sensitive to the ionic strength of the surrounding medium. Further, the excessive positive charge on the polyelectrolyte backbone leads to increase in κ with a relatively smaller slope [Fig. 2]. This decrease in conductance may be due to two factors *i.e.* dissolution of NaPSS-SAIL (aggregate) complex can lead to increase in conductivity and on the other hand, the formation of micelle saturated complexes decrease the conductivity. The *cmc* values of SAILs in NaPSS-SAIL systems increase with the increase in temperature as well as with the increase in concentration of NaPSS. This can be explained on the basis that there occurs an enhancement of the solubility of hydrophobic chains with increase in temperature that further disrupt the iceberg structure surrounding the hydrophobic chain and thus, it delays the micelle formation process in aqueous solution [51]. However, in the presence polyelectrolyte, the micelle formation is taking place at higher surfactant concentration due to the formation of NaPSS-SAIL complex, which reduces the actual amount of SAIL available for independent micellization. As can be seen from Table S1, S2 and S3 (supporting information), the β values increase with the increase in alkyl chain length of SAILs both in the absence and presence of polyelectrolyte. The comparison of the β values of SAILs in aqueous and in aqueous polyelectrolyte solution suggests that β values are relatively small in the presence of polyelectrolyte, NaPSS. This can be explained on the assumption that just before micellization or on micellization, the polyelectrolyte bound to the outer region of micelles by virtue of electrostatic interactions, leading to stabilization of micelles and resulting in decrease in β to some extent compared to that in aqueous solution. In the fluorescence measurements, beyond C_s, the dissolution of NaPSS-SAIL

(aggrgegate) complexes starts due to adsorption of excess positive charge resulting in less hydrophobic environment sensed by ANS and its fluorescence intensity decreases. This is also supported by decrease in turbidity (Fig. 4) and D_h of the NaPSS-SAIL complexes at similar concentration. After *cmc*, micelles are formed and hydrophobicity of surroundings of ANS again changes which results in increase in intensity of ANS. The transitions extracted from fluorescence technique complement well with those obtained from surface tension measurements and are listed in Table 1. The dissolution may be due to electrostatic repulsions between positively charged aggregates of SAILs adhered to polyelectrolyte backbone or dissolution via forming micelles. The various turbidity changes are shown along the turbidity profiles to justify the changes occurring on addition of SAILs (Fig. 4). Thereafter, free micelles of SAILs are formed and turbidity remains constant. In size distribution studies, beyond C_s, two bands of different D_h starts appearing along with decrease in D_h with the increase in concentration of [C_{10}mim][Cl] (Fig. 5). The appearance of two bands suggests that after charge neutralization, addition of positively charged monomers of [C_{10}mim][Cl] induces some electrostatic repulsions in already present mixed aggregates due to which some of the large aggregates break. Along with this, concentration of monomers attains a threshold value to form free micelles of [C_{10}mim][Cl]. Similar sort of variation in turbidity and size distribution has been observed in NaPSS-[C_{12}mim][Cl] and -[C_{14}mim][Cl] mixed systems. The results extracted from both of these studies are in corroboration with each other as well as with those obtained from surface tension, fluorescence and conductivity measurements. In ITC measurements, above C_s, some of the added micelles are diluted and due to electrostatic repulsions, dissolution of NaPSS-SAIL complexes also occurs. They undergo demicellization into monomers and form micelle like aggregates which results in comparatively less endothermic enthalpy changes. The enthalpograms obtained for NaPSS-[C_{10}mim][Cl] and -[C_{12}mim][Cl] mixed systems are sigmoidal in shape. In case of NaPSS-[C_{12}mim][Cl], similar sort of transitions from exothermic and endothermic heat changes have been observed and beyond *cmc*, the dilution curves obtained for both the concentrations of NaPSS (0.002% and 0.005%) merges with the dilution curve obtained in the absence of polyelectrolyte. This indicates that beyond *cmc*, the solution gets saturated with polyelectrolyte and further the presence of polyelectrolyte does not affect the micellization process of SAILs. The various concentrations regions are in line with various enthalpy changes corresponding to

various modes of interaction between NaPSS and SAILs and corroborates well with the changes observed in all the techniques discussed earlier.

4.2 Electrochemical measurements

4.2.1 Potentiometric Measurements

In order to investigate the interactions between polyelectrolyte, NaPSS and SAILs in the bulk in terms of different transitions and binding behavior of SAILs with NaPSS, potentiometric measurements using surface active imidazolium cation (C_nmim^+) based ion selective electrode (ISE) have been performed. The plots showing the variation of electromotive force (EMF) versus logarithm of concentration of $[C_{10}mim][Cl]$ in the absence and presence of NaPSS at 0.002 and 0.005% concentrations of polyelectrolyte are presented in Fig. 6(a) and for the other SAILs, plots are shown as supporting information (Fig. S9). Owing to the exquisite reproducibility of the EMF values in the absence of polyelectrolyte at different concentration of SAILs, those plots served as calibration curves. Any deviation of EMF from the calibration curve in the presence of polyelectrolyte, NaPSS indicates that the binding of SAIL with NaPSS takes place. The increase in EMF values in the presence of polyelectrolyte could be due to the reason that in NaPSS solution, some of polyelectrolyte molecules bind to the surface of membrane which reduces the potential leading to enhanced solubilization of the SAILs (cationic surfactant) present in reference solution in the membrane which produces large EMF. As can be seen from Fig. 6(a), in the presence of polymer, the potentiometric profiles show three transitions corresponding to *cac*, C_s and *cmc* of SAILs which complement well with those obtained from surface tension measurements. Initially, on the addition of SAIL, potential increases very slightly and thereafter, it increases sharply. The point of intersection of the changes gives critical aggregation concentration (*cac*) where NaPSS-SAIL (monomer) complex is formed. Beyond *cac*, EMF increases linearly with relatively smaller slope as compared to the former and gives another transition *i.e.* C_s where polyelectrolyte becomes saturated with monomers of SAILs and aggregates of SAIL are formed on the polyelectrolyte backbone. With further increasing in concentration of SAIL, EMF increases slowly before attaining a constant value after *cmc*. The concentration corresponding to different transitions obtained for NaPSS-SAILs mixed systems are presented in Table 1.

Binding Isotherm: The change in EMF values in the presence of polyelectrolyte helps to calculate the amount of SAIL bound to NaPSS molecules. The average number of SAIL monomers bound to NaPSS (v) is obtained using the following equation [52]:

$$v = \frac{[SAIL]_t - [SAIL]_f}{[NaPSS]_t} \quad (1)$$

where $[SAIL]_t$, $[SAIL]_f$ and $[NaPSS]_t$ represent total concentration of SAIL, free concentration of SAIL and the total concentration of NaPSS, respectively. Fig. 6(b) represent the binding isotherm for binding of $[C_{10}mim][Cl]$ and the corresponding plots for other SAILs are given as supporting information [Fig. S10]. The binding isotherms of SAILs with NaPSS show three characteristic regions with increasing concentration of SAILs as shown in Fig. 6(b). For $[C_{10}mim][Cl]$-NaPSS system, initially, there is very small increase in binding due to non-cooperative association between monomers of $[C_{10}mim][Cl]$ and polyelectrolyte up to concentration which is in accordance with C_2 (*cac*) as observed from different studies discussed earlier. Afterwards, in the second region, there is increase in binding to attain a plateau owing to cooperative binding among $[C_{10}mim][Cl]$ and polyelectrolyte by virtue of strong electrostatic and hydrophobic interactions and this falls between *cac* and C_s where NaPSS-SAIL (aggregate) complexes are formed and saturation of polyelectrolyte backbone takes place and later on, binding increases with a lower slope. Also, beyond C_s, the dissolution of precipitates occurs and thereafter, binding isotherm acquires constancy and SAIL free monomer concentration increases until it reaches *cmc*. The transition concentrations corresponding to different binding regions significantly correlates with other techniques studied. Similar kind of binding isotherms are obtained for NaPSS-$[C_{12}mim][Cl]$ and -$[C_{14}mim][Cl]$ mixed systems.

4.2.2 Voltammetric Measurements

In the voltammetric studies, TEMPO is used as an electroactive probe which distributes itself between aqueous and micellar phase. The voltammetric measurements are performed in two ways. The cyclic voltammetric (CV) studies are carried out to find the micellar diffusion coefficient (D_m) of the pure and mixed systems and the interactions between polyelectrolyte and SAILs have been investigated using differential pulse voltammetry (DPV). There are no literature reports dealing with the DPV studies of mixed systems comprising polymer and

surfactants. The voltammogram of TEMPO (2 mM) shows a pair of reversible oxidation and reduction peaks using Pt as working electrode and 0.1 M KCl as a supporting electrolyte. The separation between the anodic and cathodic peak potentials was 59 mV which suggests that process involves reversible oxidation and reduction of $1e^-$. The voltammograms of TEMPO in micellar solution of [C_{10}mim][Cl] (400 mM) at different scan rates varying from 10 to 100 mV/s is shown in Fig. 7(a) and the corresponding plots for other SAILs and NaPSS-SAIL mixed systems are shown in supporting information [Fig. S11(a) and Fig. S12(a)]. The variation of current has been found to be linear with no shift in peak potential which suggests that process is diffusion controlled and provides basis to determine diffusion coefficient for the pure and mixed systems using Randles-Sevcik equation [53] which relates peak current (i_p) with scan rates ($v^{1/2}$) using the relation:

$$i_p = 0.4463\, FAC\, (F/RT)^{1/2}\, v^{1/2}\, {D_m}^{1/2} \quad (2)$$

where, A, F, and C are area of electrode, Faraday's constant and concentration of electroactive species, respectively. The other terms have their usual meanings. The slopes of linear plots of i_p versus $v^{1/2}$ for the investigated NaPSS-[C_{10}mim][Cl], -[C_{12}mim][Cl], and -[C_{14}mim][Cl] mixed systems are shown in inset of Fig. 7(a), S11(a) and S12(a) respectively, which give the value of diffusion coefficients for the proposed systems. The obtained values of diffusion coefficients are listed in Table S5 (supporting information). The diffusion of electroactive probe, TEMPO depends on its distribution among micellar and aqueous phases. TEMPO, being hydrophobic in nature, preferably gets solubilized in micellar phase and thus, the obtained values of diffusion coefficients correspond to those of micelles. In the present systems, the D_m values increase with the increase in alkyl chain length of SAILs and it is in accordance with literature reports [54]. Their values decrease with the increase in concentration of polyelectrolyte, NaPSS from 0.002 to 0.005%. The variation in D_m values can be interpreted on the grounds of two effects, *i.e.* obstruction effect and hydration effect [55]. With the increase in alkyl chain length, the hydrophobicity increases leading to decrease in hydration and it ultimately result in faster diffusion. On the other hand, with the increase in concentration of NaPSS from 0.002 to 0.005%, the values of D_m decreases again due to hydration effect and water solvation

around NaPSS-SAIL aggregates demobilized the structured layer of water and thus, it is responsible for the decrease in diffusion coefficient.

An another study has also been performed using cyclic voltammetry in which D_m values are obtained at various micellar concentrations of SAILs in the interest of getting inter-micellar interaction parameter (k_d) and self diffusion coefficient (D^0_m) in the absence of inter-micellar interactions. These parameters are obtained using the equation [56].

$$D_m = D_m^0/[1 + k_d(C_s - cmc)] \quad (3)$$

where C_s denotes the total concentration of SAIL. Using the values of slope and intercept from the plot of 1/ D_m versus C_s-*cmc*, D^0_m and k_d values are extracted for all the NaPSS-SAILs mixed systems at 0.002% and 0.005% concentrations of polyelectrolyte and the values are given in Table S5 (supporting information). The D_m values decrease with the increase in concentration of SAILs in all mixed systems which are in accordance with the literature [57, 58] during exploring the self diffusion coefficient values of micelles. The value of inter-micellar interaction parameter (k_d) is highest for [C_{14}mim][Cl] among the three SAILs studied and is influenced by polyelectrolyte concentration. The self diffusion coefficient values, D^0_m are maxima for pure systems and it decreases in the presence of NaPSS in the investigated NaPSS-SAIL mixed systems.

The differential pulse voltammograms for 0.005 % NaPSS-[C_{10}mim][Cl] mixed system is shown in Fig. 7(b) and the corresponding variation of i_p versus concentration is presented in the inset. The plots for NaPSS-SAIL mixed systems at 0.002 and 0.005% concentration are given in supporting information [Fig. S11(b) and Fig. S12(b)]. The voltammograms of all investigated mixed systems show two transitions corresponding to C_s and *cmc* which matches with those obtained from other techniques in contrast with three transitions as observed in other studies. In premicellar region, only monomers of SAIL are present which does not offer highly hydrophobic environment for the solubilization of probe and thus, leading to weak interactions between electroactive probe and the monomers of SAIL. Therefore in this concentration region, the interactions between NaPSS and SAILs could not be proved using differential pulse voltammetry, however, the interactions between NaPSS and SAILs in this concentration regime prevails as supported by different studies. With increase in concentration of respective SAIL, no

transition corresponding to C_2 (*cac*) was observed from voltammetric measurements indicating the non-formation of any hydrophobic domains in polymer-SAIL (monomer) complex at the sensing level of TEMPO. After that, on further addition of SAIL, peak current (i_p) starts decreasing with lower slope to a concentration corresponding to C_s. After Cs, the micelle formation takes place which enhances the solubilization of TEMPO in the stern layer of micelle leading to instantaneous decrease in i_p and then tending to constant value in the micellar phase. The concentration at which sharp decrease in i_p occurs gives the value of *cmc*. The obtained values of *cmc* for all studied systems are shown in Table 1. The *cmc* values of pure SAILs are found to be in good agreement with the literature reports as well as with those obtained from other techniques employed. For NaPSS-SAILs systems, on increasing the concentration of polyelectrolyte, the minima shifts to higher concentration and also gives the low value of current. This is due to the reason that initially when polyelectrolyte molecules are present in TEMPO, although NaPSS is present in a very low concentration; it might be possible that some small sort of interaction could take place between NaPSS and TEMPO which ultimately liable for overall less current changes in all mixed systems of NaPSS and SAILs.

It has been observed that the relative hydrophobicity of the respective SAILs in terms of their alkyl chain length along with electrostatic interactions govern their interactions with oppositely charged NaPSS. Both the interfacial and bulk properties of the potentially useful NaPSS can be modified and tuned in the presence of SAILs. On the other hand, the amount of NaPSS in mixture is also found to exert remarkable effect on the colloidal properties of solution in the presence of different SAILs. The binding among NaPSS and SAILs has been characterized in terms of different concentration regimes along with variety of physicochemical properties employing different techniques and the results complement well each other.

3.6. Conclusions

The present report has explored the effect of anionic polyelectrolyte, Poly sodium 4-styrene sulphonate (NaPSS) on the aggregation and micellization behavior of surface active based ionic liquids (SAILs) using various techniques. The surface tension data shows complex behavior that demonstrates the adsorption of polyelectrolyte and SAILs at the interface along with their subsequent desorption. The surface adsorption is highly influenced by the chain length

of SAILs as it is clear from the different tensiometric profiles of SAILs in the presence of NaPSS. The *cmc* values of SAILs obtained from all the techniques increases in the presence of polyelectrolyte which clearly conform the complexation between NaPSS and SAIL monomers and thus, more number of SAIL monomers are required for independent micellization. Thermodynamic parameters calculated using conductivity indicates that micelle formation process is entropy controlled over the whole temperature studied. The macroscopic changes occurring in the aggregate sizes produce changes in hydrodynamic diameter and turbidity profiles which permits us to monitor the degree of complex formation. The binding studies are performed using potentiometric PVC sensor for alkyl imidazolium ions and found that binding between anionic polyelectrolyte and cationic SAILs is uncooperative in lower concentration regions and highly cooperative in higher concentration regimes due to strong electrostatic and hydrophobic interactions. The results obtained from potentiometric studies strongly correlates with the results extracted from surface tension, fluorescence, and conductivity measurements. Using CV technique, important parameters like D_m, D^0_m, and k_d were anticipated. The values of diffusion coefficient have been found to be influenced by the chain length of SAILs as well as with increase in concentration of polyelectrolyte and show a decrease with increase in chain length of SAILs.

Acknowledgement

This work was financially supported by the Department of Science and Technology (DST) New Delhi, India as a part of Project NO.SR/S1/PC-02/2011. Renu Sharma is thankful to University Potential for Excellence (UPE) scheme, Guru Nanak Dev University, Amritsar for the award of research fellowship (RF).

References

1. B.S. Kim, T.H. Fan, O.V. Lebedeva, O.I. Vinogradova, *Macromolecules*, 2005, 38, 8066-8070.
2. B. Jonsson, B. Lindman, K. Holmberg, B. Kronberg, *Surfactants and Polymers in Aqueous Solution,* John Wiley & Sons, 1998..
3. C. Wang, K.C. Tam, *Langmuir*, 2002, 18, 6484-6490.
4. J. Fundin, P. Hansson, W. Brown, I. Lidegran, *Macromolecules*, 1997, 30, 1118-1126.
5. S. Llamas, E. Guzmán, F. Ortega, N. Baghdadli, C. Cazeneuve, R.G. Rubio, G.S. Luengo, *Adv. Colloid Interface Sci.*, 2015, doi:10.1016/j.cis.2014.05.007.
6. Y. Pi, Y. Shang, C. Peng, H. Liu, Y. Hu, J. Jiang, *J. Colloid Interface Sci.*, 2006, 301, 631-636.
7. A. Dan, S. Ghosh, S.P. Moulik, *Carbohyd. Polym*., 2010, 80, 44-52.
8. G. Petzold, V. Dutschk, M. Mende, R. Miller, *Colloid Surf. A*, 2008, 319, 43-50.
9. J. Han, F. Cheng, X. Wang, Y. Wei, *Carbohyd. Polym.*, 2012, 88, 139-145.
10. J. Mata, J. Patel, N. Jain, G. Ghosh, P. Bahadur, *J. Colloid Interface Sci.*, 2007, 297, 797-804.
11. E. Staples, L. Tucker, J. Penfold, N. Warren, R.K. Thomas, D.J.F. Taylor, *Langmuir*, 2002, 18, 5147-5153.
12. P.M. Macdonald, Jr. A.Tang, *Langmuir*, 1997, 13, 2259-2265.
13. M. Almgrem, P. Hansson, E. Mukhtar, J.V. Stam, *Langmuir*, 1992, 8, 2405-2412.
14. D.J.F. Taylor, R.K. Thomas, J.D. Hines, K. Humphreys, J. Penfold, *Langmuir*, 2002, 18, 9783-9791.
15. C. Brinatti, L.B. Mello, W. Loh, *Langmuir*, 2014, 30, 6002-6010.
16. H. Wang, Y. Wang, *J. Phys. Chem. B*, 2010, 114, 10409-10416.
17. K. Kogej, J. Skerjanc, *Langmuir*, 1999, 15, 4251-4258.
18. Z. Li, Z. Liu, J. Zhang, B. Han, J. Du, Y. Gao, T. Jiang, *J. Phys. Chem. B*, 2005, 109, 14445-14448.
19. M. Blesic, M.H. Marques, N.V. Plechkova, K.R. Seddon, L.P.N. Rebelo, A. Lopes, *Green Chem.*, 2007, 9, 481-490.
20. J. Bowers, C.P. Butts, P.J. Martin, M.C. Vergara Gutierrez, *Langmuir*, 2004, 20, 2191-2198.

21. J. Wang, H. Wang, S. Zhang, H. Zhang, Y. Zhao, *J. Phys. Chem. B*, 2007, 111, 6181-6188.
22. T.J. Trivedi, K.S. Rao, T. Singh, S.K. Mandal, N. Sutradhar, A.B. Panda, A. Kumar, *ChemSusChem*, 2011, 4, 604-608.
23. B. Dong, N. Li, L. Zheng, L. Yu, T. Inoue, *Langmuir*, 2007, 23, 4178-4182.
24. J. Liu, M. Zhao, Q. Zhang, D. Sun, X. Wei, L. Zheng, *Colloid Polym. Sci*., 2011, 289, 1711-1718.
25. P. Bharmoria, T. Kang, A. Kumar, *J. Colloid Interface Sci.*, 2013, 407, 361-369.
26. R. Sanan, T. Kang, R.K. Mahajan, *Phys. Chem. Chem. Phys*., 2014, 16, 5667-5677.
27. S. Mahajan, R. Sharma. R.K. Mahajan, *Colloid Surf. A*, 2013, 424, 96-104.
28. P.M. Reddy, P. Venkatesu, *J. Colloid Interface Sci.*, 2014, 420, 166-173.
29. T. Singh, P. Bharmoria, M. Morikawa, N. Kimizuka, A. Kumar, *J. Phys. Chem. B*, 2012, 116, 11924-11935.
30. J. Liu, L. Zheng, D. Sun, X. Wei, *Colloid Surf. A*, 2010, 358, 93-100.
31. Q. Zhang, W. Kang, D. Sun, J. Liu, X. Wei, *Appl. Surf. Sci.*, 2013, 279, 353-359.
32. B. Das, D. Ray, R. De, *Carbohyd. Polym*., 2014, 113, 208-216.
33. B. Dong, N. Li, L. Zheng, L. Yu, T. Inoue, *Langmuir*, 2007, 23, 4178-4182.
34. O.A. El Seoud, P.A.R. Pires, T. Abdel-Moghny, E.L. Bastos, *J. Colloid Interface Sci*., 2007, 313, 296-304.
35. C. Monteux, C. E. Williams, V. Bergeron, *Langmuir*, 2004, 20, 5367-5374.
36. E. Guzman, H. Ritacco, F. Ortega, T. Svitova, C.J. Radke, R.G. Rubio, *J. Phys. Chem. B*, 2009, 113, 7128-7137.
37. A. Klebanau, N. Kliabanova, F. Ortega, F. Monroy, R.G. Rubio, V. Starov, *J. Phys. Chem. B*, 2005, 109, 18316-18323.
38. B. Dong, X.Y. Zhao, L.Q. Zheng, J. Zhang, N. Li, T. Inoue, *Colloids Surf. A*, 2008, 317, 666-672.
39. P.C. Shanks, E.I. Franses, *J. Phys. Chem.*, 1992, 96, 1794-1805.
40. R. Sharma. S. Mahajan, R.K. Mahajan, *Colloid Surf. A*, 2013, 427, 62-75.
41. P.C. Griffiths, N. Hirst, A. Paul, S.M. King, R.K. Heenam, R. Farley, *Langmuir*, 2004, 20, 6904-6913.
42. K.C. Tam, E.W. Jones, *Chem. Soc. Rev*., 2006, 35, 693-709.

43. P. Hansson, S. Schneider, B. Lindman, *J. Phys. Chem. B*, 2002, 106, 9777-9793.
44. B. Magny, I. Ilipoulos, R. Zana, R. Audebert, *Langmuir*, 1994, 10, 3180-3187.
45. N. Jain, S. Trabelsi, S. Guillot, D. McLoughin, D. Langevin, P. Letellier, M. Turmine, *Langmuir*, 2004, 20, 8496-8503.
46. D. Mitra, S.C. Bhattacharya, S.P. Moulik, *J. Phys. Chem. B*, 2008, 112, 6609-6619.
47. D.J.F. Taylor, R.K. Thomas, P.X. Li, J. Penfold, *Langmuir*, 2003, 19, 3712-3719.
48. H. Pan, P.Y. Chen, H.X. Liu, Y. Chen, Y.P. Wei, M.J. Zhang, F. Cheng, *Carbohyd. Polym.*, 2012, 89, 899-905.
49. H. Kang, B. Peng, Y. Liang, X. Han, H. Liu, *J. Colloid Interface Sci.*, 2009, 333, 135-140.
50. Z. Gao, J.C.T. Kwak, R.E. Wasylichen, *J. Colloid Interface Sci*., 1988, 126(1), 371-376.
51. Y. Wei, F. Wang, Z. Zhang, C. Ren, Y. Lin, *J. Chem. Eng. Data*, 2014, 59, 1120-1129.
52. A.K. Bordbar, A. Taheri-Kafrani, *Colloids Surf. B*, 2007, 55, 84-89.
53. K. Chokshi, S. Qutubuddin, A. Hussam, *J. Colloid Interface Sci.*, 1989, 129, 315-326.
54. R.K. Mahajan. N. Kaur, M.S. Bakshi, *Colloids Surf. A*, 2006, 276, 221–227
55. R.K. Mahajan. J. Chawla, M.S. Bakshi, *Colloids Surf. A*, 2004, 237, 119-124.
56. A.B. Mandal, B.U. Nair, *J. Phys. Chem*., 1991, 95, 9008-9013.
57. A.B. Mandal, *Langmuir*, 1993, 9, 1932-1933.
58. J. James, C. Ramalechume, A.B. Mandal, *Chem. Phys. Lett*., 2005, 405, 84-89.

Figure Captions

Scheme 1 Molecular Structures of (a) 1-alkyl-3-methyl imidazolium chloride (SAIL) (b) Polyelectrolyte, Poly sodium 4-styrene sulphonate (NaPSS).

Scheme 2 Schematic presentation of binding interactions between polyelectrolyte (NaPSS) and surface active ionic liquids (SAILs)

Fig.1 (a) Variation of surface tension (γ) as a function of logarithm of concentration of three SAILs at 0.002% concentration of NaPSS (b) Variation of surface tension (γ) as a function of logarithm of concentration of $[C_{10}mim][Cl]$ at 0.002 and 0.005% concentration of NaPSS.

Fig.2 Variation of specific conductivity (κ) as a function of concentration of $[C_{10}mim][Cl]$ in the presence of (a) 0.002% and (b) 0.005% NaPSS at different temperatures.

Fig.3 (a) Fluorescence intensity of ANS in 0.002% NaPSS solution as a function of concentration of SAILs (b) fluorescence intensity of ANS in aqueous and aqueous NaPSS solutions at 0.002 and 0.005% concentrations as a function of concentration of $[C_{10}mim][Cl]$.

Fig.4 (a) Variation of turbidity versus concentration of three SAILs in polyelectrolyte (NaPSS) solution at a concentration of 0.002%; (c) Variation of turbidity versus concentration of $[C_{10}mim][Cl]$ in the presence of 0.002 and 0.005% concentrations of NaPSS.

Fig.5 Size distributions for 0.002% concentration of NaPSS in the presence of increasing concentrations of (a) $[C_{10}mim][Cl]$, (b) $[C_{12}mim][Cl]$ and (c) $[C_{14}mim][Cl]$. (d) Variation of hydrodynamic diameter (D_h) as a function of concentration of SAILs in 0.002% NaPSS.

Fig.6 (a) EMF as a function of logarithm of concentration of $[C_{10}mim][Cl]$ in the absence and presence of 0.002 and 0.005% NaPSS.(b) Binding isotherms of v versus logarithm of concentration of $[C_{10}mim][Cl]$ in the presence of 0.002 and 0.005% NaPSS.

Fig.7 (a) Reversible cyclic voltammograms of TEMPO (2 mM) in supporting electrolyte KCl (0.1 M) in micellar solution of $[C_{10}mim][Cl]$ at different scan rates in the presence of 0.005% NaPSS [Inset of plot gives the variation of i_p (A) versus $v^{1/2}$ $(V\ s^{-1})^{1/2}$ for TEMPO ion in aqueous $[C_{10}mim][Cl]$ solution and in the presence of NaPSS] and (b) Differential pulse voltammograms (DPV) of TEMPO (2mM) in supporting electrolyte KCl (0.1 M) for varying concentrations of $[C_{14}mim][Cl]$ in the presence of 0.005% NaPSS [Inset of plot gives the variation of i_p as a function of $[C_{10}mim][Cl]$ in aqueous and aqueous NaPSS solution (0.002 and 0.005%).

Table 1 Interaction characteristic concentrations C_1, C_2, C_3 and C_4 (mmol dm^{-3}) observed from surface tension (S.T.), fluorescence (Flu.), potentiometry, turbidity (Turb.), conductance (Cond.) and differential pulse voltammetry (DPV) measurements of SAILs in the absence and presence of polyelectrolyte NaPSS (0.002 and 0.005%) at 298.15K.

		S.T.	Flu.	Potentiometry	Turb.	Cond.	DPV
[C_{10}mim][Cl]	*cmc*	27.7	33.4	39.0	-	33.5	41.3
[C_{10}mim][Cl]+0.002%	C_1	-	-	-	-	-	-
	C_2 (*cac*)	1.56	2.50	2.55	8.20	3.20	-
	C_3 (C_s)	8.00	21.1	18.5	21.3	-	12.8
	C_4 (*cmc*)	30.8	49.3	44.6	44.8	35.5	43.4
[C_{10}mim][Cl]+0.005%	C_1	-	-	-	-	-	-
	C_2 (*cac*)	1.61	3.00	2.63	7.10	3.50	-
	C_3 (C_s)	10.5	23.2	24.5	22.4	-	16.1
	C_4 (*cmc*)	32.3	48.4	49.5	46.0	37.4	49.5
[C_{12}mim][Cl]	*cmc*	13.8	12.0	15.0	-	12.1	12.0
[C_{10}mim][Cl]+0.002%	C_1	0.53	0.57	-	-	-	-
	C_2 (*cac*)	5.08	-	1.00	3.00	1.23	-
	C_3 (C_s)	5.98	3.00	5.37	7.00	-	4.30
	C_4 (*cmc*)	13.1	14.4	16.8	14.1	12.9	17.2
[C_{10}mim][Cl]+0.005%	C_1	0.55	0.58	-	-	-	-
	C_2 (*cac*)	5.25	-	1.23	2.50	1.30	-
	C_3 (C_s)	8.16	3.70	6.44	7.50	-	4.20
	C_4 (*cmc*)	13.5	17.7	17.4	14.7	13.1	15.0
[C_{14}mim][Cl]	*cmc*	3.10	2.80	3.30	-	2.80	5.00
[C_{14}mim][Cl]+0.002%	C_1	0.02	0.08	-	-	-	-
	C_2 (*cac*)	0.04	-	0.10	0.68	0.30	-
	C_3 (C_s)	0.14	0.31	0.27	1.55	-	0.79
	C_4 (*cmc*)	1.90	3.30	3.50	3.18	3.00	6.30
[C_{14}mim][Cl]+0.005%	C_1	0.02	0.09	-	-	-	-
	C_2 (*cac*)	0.12	-	0.12	0.53	0.46	-
	C_3 (C_s)	0.22	0.32	0.35	1.58	-	1.20
	C_4 (*cmc*)	2.60	3.70	3.70	3.36	3.10	7.00

The error estimate in *cmc* is ±0.10 mmol dm^{-3}

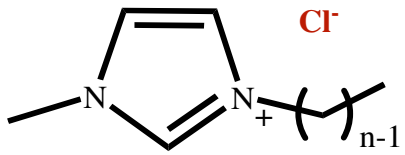

(n = 10, 12, 14)

(a)

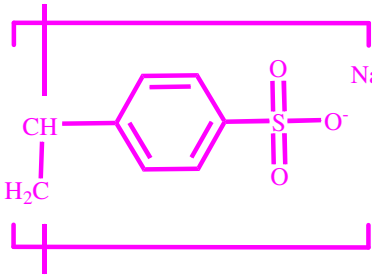

(b)

Scheme 1

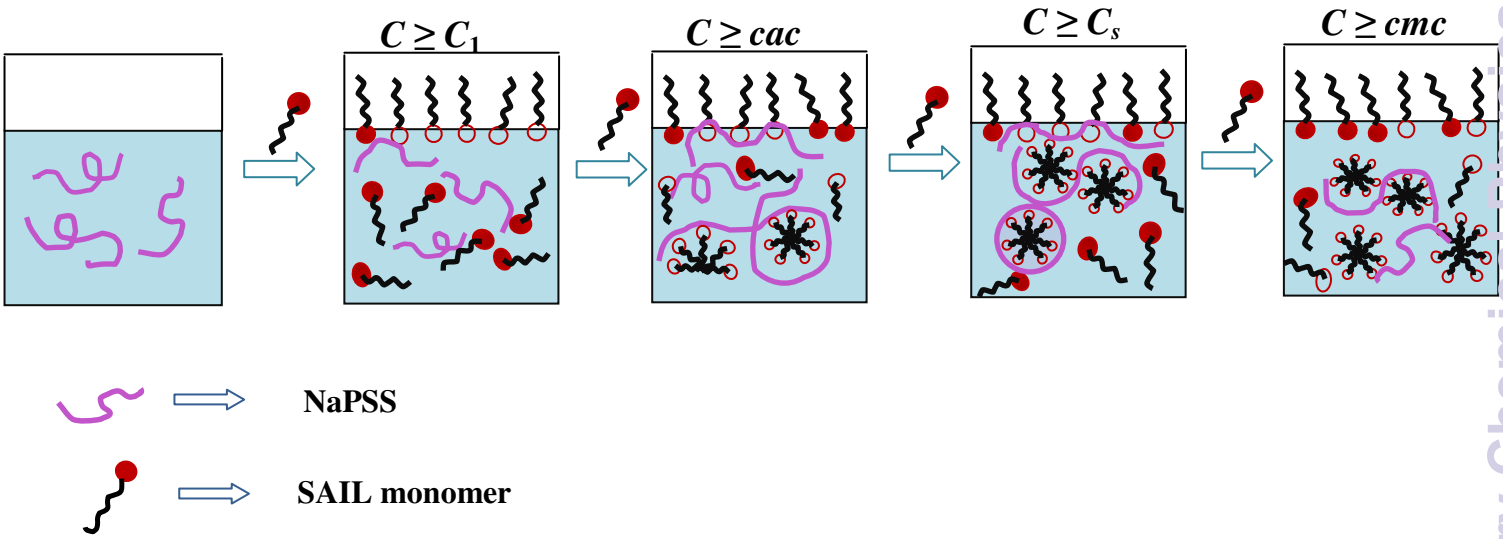

Scheme 2

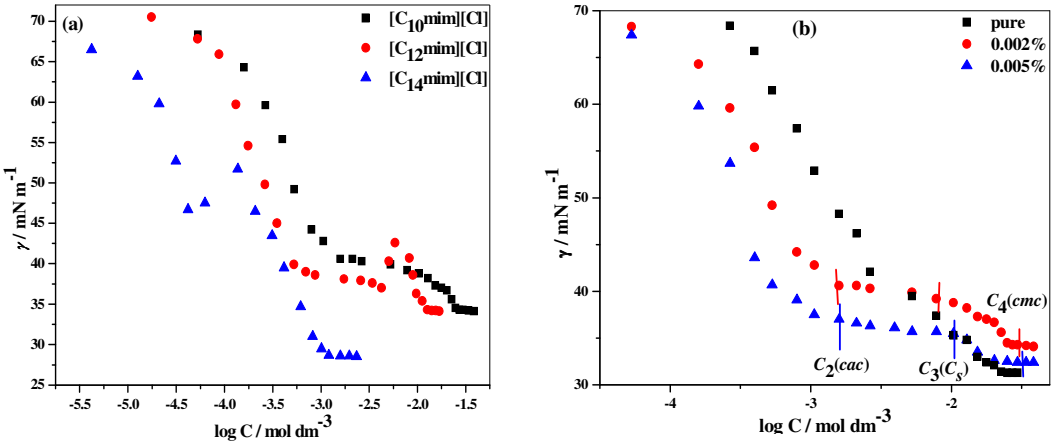

Fig.1

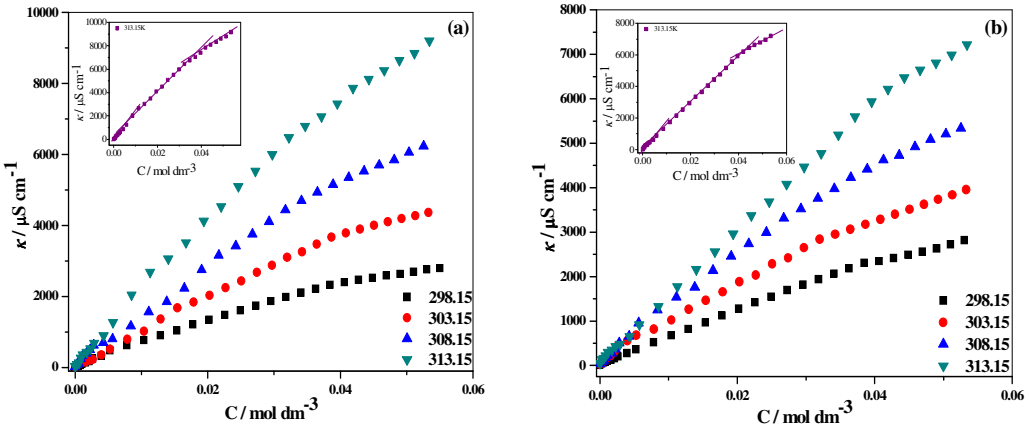

Fig.2

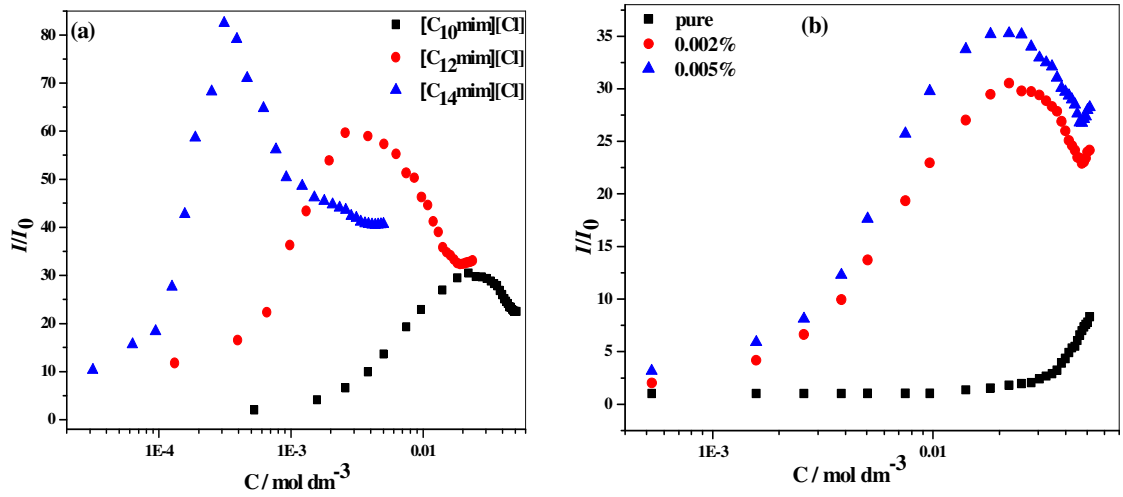

Fig.3

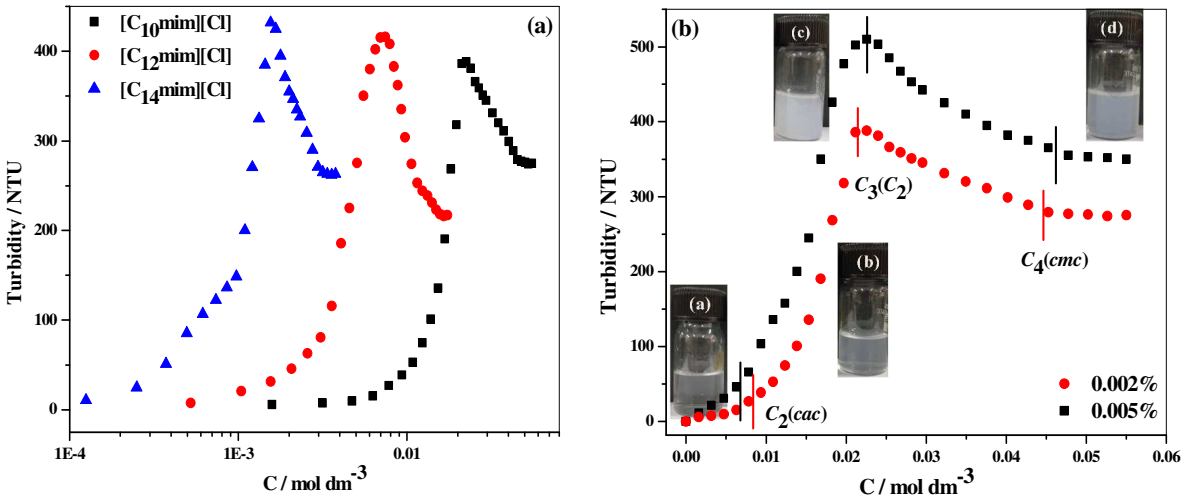

Fig.4

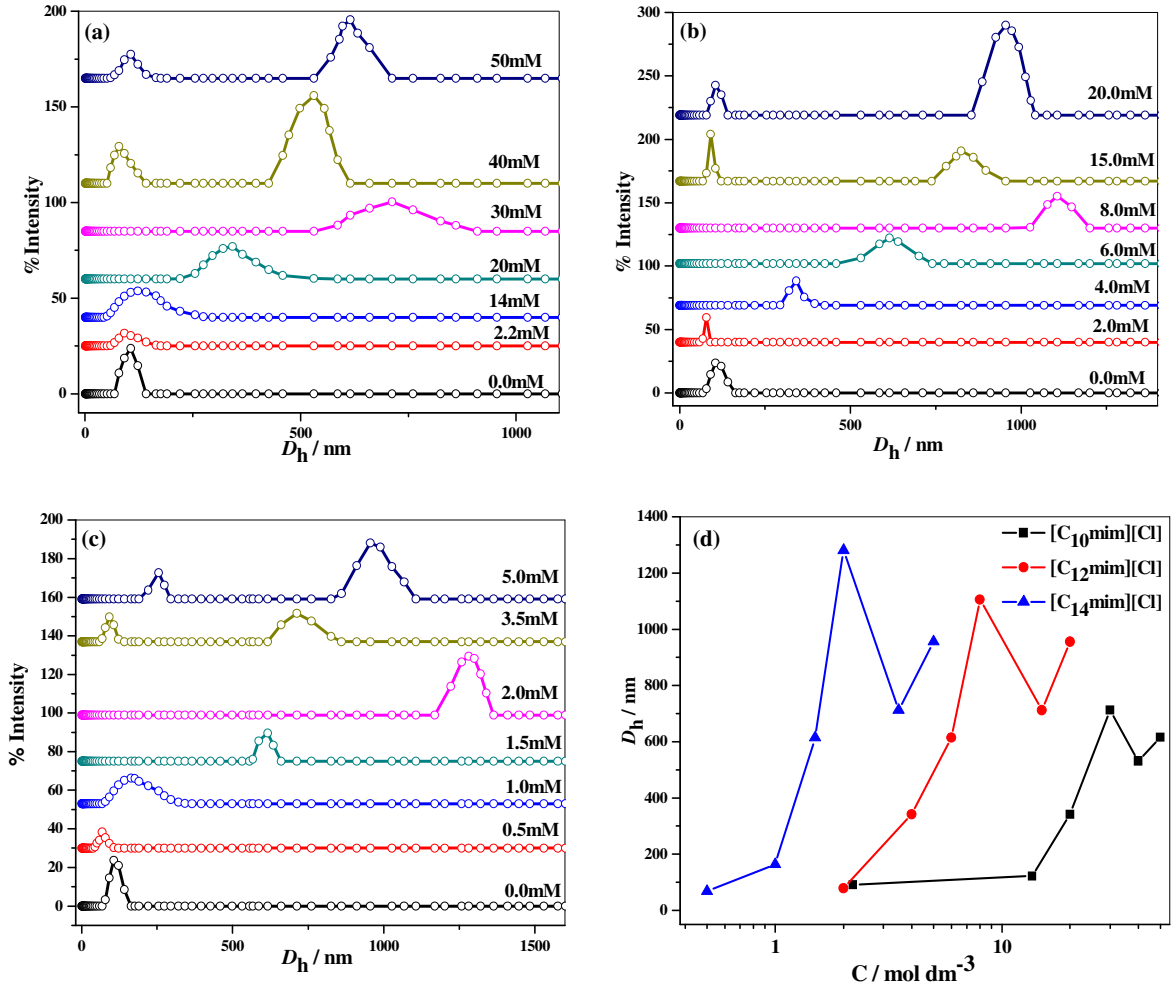

Fig.5

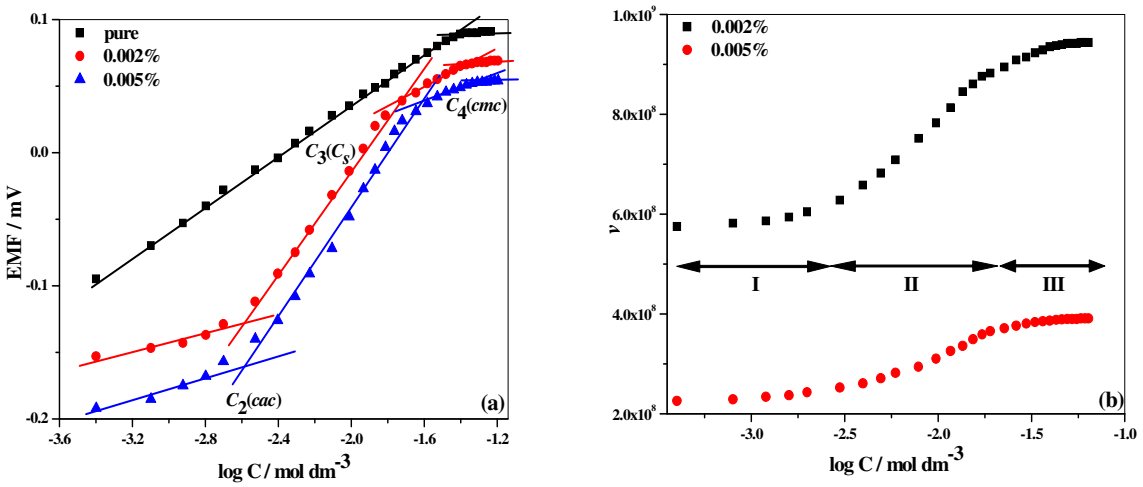

Fig.6

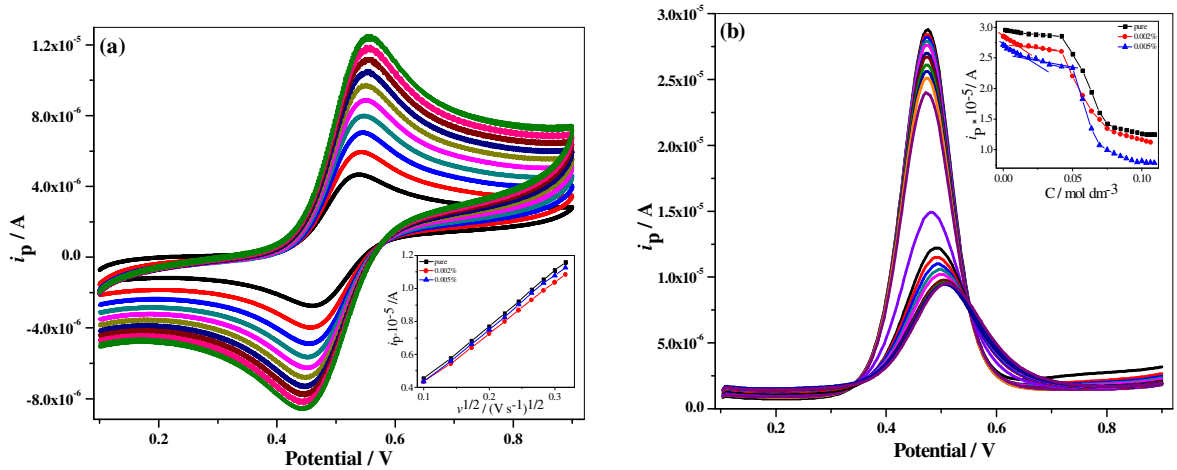

Fig.7